Progress in Oceanography 177 (2019) 101873

Contents lists available at ScienceDirect

Progress in Oceanography

journal homepage: www.elsevier.com/locate/pocean

Plankton community respiration and bacterial metabolism in a North Atlantic Shelf Sea during spring bloom development (April 2015)

E. Elena García-Martín[a,*], Chris J. Daniels[b], Keith Davidson[c], Jose Lozano[d], Kyle M.J. Mayers[b,e], Sharon McNeill[c], Elaine Mitchell[c], Alex J. Poulton[b,f], Duncan A. Purdie[e], Glen A. Tarran[g], Callum Whyte[c], Carol Robinson[a]

[a] Centre for Ocean and Atmospheric Sciences, School of Environmental Sciences, University of East Anglia, Norwich Research Park, Norwich NR4 7TJ, UK
[b] Ocean Biogeochemistry and Ecosystems, National Oceanography Centre, Waterfront Campus, European Way, Southampton SO14 3ZH, UK
[c] Scottish Association for Marine Science, Scottish Marine Institute, Oban, Argyll, PA371QA Scotland, UK
[d] Departamento Ecología y Biología animal/ECIMAT, Facultad de Ciencias del Mar, Universidad de Vigo, CP 36210 Vigo, Spain
[e] Ocean and Earth Science, University of Southampton, National Oceanography Centre Southampton, Southampton SO14 3ZH, UK
[f] The Lyell Centre, Heriot-Watt University, Edinburgh, UK
[g] Plymouth Marine Laboratory, Prospect Place, Plymouth PL1 3DH, UK

ARTICLE INFO

Keywords:
Plankton community respiration
Bacterial metabolism
Bacterial growth efficiencies
Celtic Sea
Spring bloom

ABSTRACT

Spring phytoplankton blooms are important events in Shelf Sea pelagic systems as the increase in carbon production results in increased food availability for higher trophic levels and the export of carbon to deeper waters and the sea-floor. It is usually accepted that the increase in phytoplankton abundance and production is followed by an increase in plankton respiration. However, this expectation is derived from field studies with a low temporal sampling resolution (5–15 days). In this study we have measured the time course of plankton abundance, gross primary production, plankton community respiration, respiration of the plankton size classes (> 0.8 μm and 0.2–0.8 μm) and bacterial production at ≤5 day intervals during April 2015 in order to examine the phasing of plankton autotrophic and heterotrophic processes. Euphotic depth-integrated plankton community respiration increased five-fold (from 22 ± 4 mmol O_2 m^{-2} d^{-1} on 4th April to 119 ± 4 mmol O_2 m^{-2} d^{-1} on 15th April) at the same time as gross primary production also increased five-fold, (from 114 ± 5 to 613 ± 28 mmol C m^{-2} d^{-1}). Bacterial production began to increase during the development of the bloom, but did not reach its maximum until 5 days after the peak in primary production and plankton respiration. The increase in plankton community respiration was driven by an increase in the respiration attributable to the > 0.8 μm size fraction of the plankton community (which would include phytoplankton, microzooplankton and particle attached bacteria). Euphotic depth-integrated respiration of the 0.2–0.8 μm size fraction (predominantly free living bacteria) decreased and then remained relatively constant (16 ± 3 – 11 ± 1 mmol O_2 m^{-2} d^{-1}) between the first day of sampling (4th April) and the days following the peak in chlorophyll-*a* (20th and 25th April). Recent locally synthesized organic carbon was more than sufficient to fulfil the bacterial carbon requirement in the euphotic zone during this productive period. Changes in bacterial growth efficiencies (BGE, the ratio of bacterial production to bacterial carbon demand) were driven by changes in bacterial production rates increasing from < 30 ± 14% on 4th April to 51 ± 11% on 25th of April. This study therefore shows a concurrent rather than a phased increase in primary production and community respiration attributable to cells > 0.8 μm during the development of the spring bloom, followed 5 days later by a peak in bacterial production. In addition, the size fractionated respiration rates and high growth efficiencies suggest that free living bacteria are not the major producers of CO_2 before, during and a few days after this shelf sea spring phytoplankton bloom.

1. Introduction

Reduced water column turbulence is one of the principal factors governing the rapid increase in plankton abundance in western-European shelf seas, such as the Celtic Sea, during spring (Pingree et al., 1976; Fasham et al., 1983; Taylor et al., 1997; Smyth et al., 2014). The

* Corresponding author.
E-mail address: enmagarciamartin@gmail.com (E.E. García-Martín).

https://doi.org/10.1016/j.pocean.2017.11.002

Available online 04 November 2017

increase in water column stability, the presence of high nutrient concentrations and ample light in the surface mixing layer trigger an increase in primary production, and therefore an increase in phytoplankton abundance (Joint et al., 2001; Behrenfeld, 2010). Most of the studies of temperate spring "blooms" of phytoplankton focus on the rapid increase in primary production and the succession of phytoplankton groups (Joint et al., 1986; Widdicombe et al., 2010; Fileman et al., 2011; Barnes et al., 2015; Daniels et al., 2015). Only two studies have measured both plankton production and plankton respiration during a spring bloom with the temporal resolution (≤1 week) required to discern the short term phasing between primary production and respiration (Blight et al., 1995; Caffrey et al., 1998). These studies in coastal waters of the UK (Blight et al., 1995) and the USA (Caffrey et al., 1998) showed a time lag of 5–15 days between the maximum rate of primary production and the maximum rate of community respiration. Blight et al. (1995) explained the delay in the respiration response to be due to the time required for phytoplankton derived dissolved organic matter (DOM) to become available to the bacteria.

DOM exuded by phytoplankton or made available by zooplankton sloppy feeding is composed of high- and low-molecular weight compounds (Lancelot, 1984; Biddanda and Benner, 1997). High molecular weight compounds are easily and rapidly assimilated by bacteria (Amon and Benner, 1994). Therefore, production of high molecular weight compounds could stimulate an increase in heterotrophic bacterial respiration and production on short time scales of hours to days as observed in microcosm addition experiments (Amon and Benner, 1994, 1996; Lønborg et al., 2016). This concurrent increase in primary production and bacterial production has also been observed in a spring bloom study which sampled at daily intervals (Ducklow et al., 1993). However, due to logistics, the sampling frequency in natural field studies is usually greater than this (i.e. weeks rather than hours - days) and this longer sampling interval could miss the concurrent increase in phytoplankton production and bacterial activity.

The activity of the microbial foodweb alters the biochemical composition of the phytoplankton derived dissolved and particulate organic matter (Fernández et al., 1992; Grossart et al., 2006; Danger et al., 2007), which then influences bacterial growth efficiencies (BGE, the ratio of bacterial production to bacterial carbon demand) and in the long term, the balance between production of CO_2, transfer of carbon to higher trophic groups and export and storage of carbon in deeper waters. Despite the importance of understanding the temporal variability in bacterial growth efficiency to quantification of the cycling of carbon, there have been no previous measurements of BGE on temporal scales < 1 week during spring bloom events.

The aim of this study is to explain the temporal evolution of plankton community respiration and bacterial metabolism (production, respiration and the bacterial growth efficiency) during a spring bloom event at a shelf sea station and to determine the phasing between these processes and primary production at short temporal scales (≤5 days). A companion paper in this special issue incorporates these spring time data into a broader synthesis of the annual and spatial variability in plankton dynamics of the Celtic Sea (García-Martín et al., this issue).

2. Material and methods

2.1. Study site and sampling procedure

A four week study was conducted during April 2015 at a single station in the centre of the Celtic Sea (Central Celtic Sea, CCS, 49.39°N, 8.58°W, Fig. 1) where the water depth was approximately 147 m. Depth profiles of temperature and salinity were measured using a conductivity-temperature-depth (CTD) profiler (Sea-Bird Electronics, Washington, USA). Water samples were collected pre-dawn (~03:00 GMT) from 7 depths on each of 6 occasions (4th, 6th, 11th, 15th, 20th, 25th April) with 20-L Niskin bottles mounted on a rosette sampling frame to which the CTD was attached. Six of these sample depths were in the

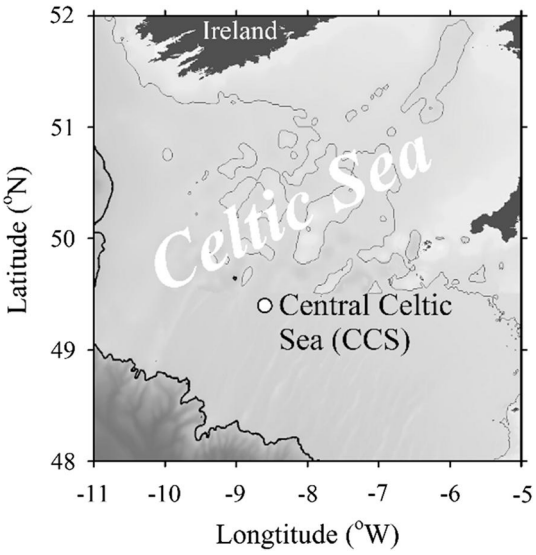

Fig. 1. Location of the Central Celtic Sea sampling station in the Celtic Sea.

euphotic zone, considered as the depth at which incident irradiance is 1% of surface irradiance, (60, 40, 20, 10, 5 and 1% of surface irradiance; Poulton et al., this issue), and one sample depth was below the euphotic zone at 70 m. Seawater was carefully transferred from each of the Niskin bottles into 10 L carboys for subsequent determination of plankton community respiration derived from both dissolved oxygen consumption and the reduction of 2-(ρ-iodophenyl)-3-(ρ-nitrophenyl)-5phenyl tetrazolium chloride (INT). The INT reduction method does not directly measure respiration (Maldonado et al., 2012), but is a good proxy to estimate plankton and bacterial respiration over short time scales (Martínez-García et al., 2009; Aranguren-Gassis et al., 2012; García-Martín et al., 2016). Water samples for the determination of chlorophyll-*a* (Chl-*a*), gross primary production (PP), heterotrophic bacterial production (BP) and bacterial abundance (BA) were taken from the same Niskin bottles as the samples collected for the determination of plankton community respiration. Sampling procedures followed Poulton et al. (2016) for Chl-*a* (see also Hickman et al., this issue) and primary production (see also Poulton et al., this issue), and Tarran et al. (2006) for bacterial abundance (see also Tarran et al., this issue).

2.2. Nutrients, total chlorophyll a, primary production and dissolved organic carbon production

Nitrate + nitrite and phosphate concentrations were analysed on board using a Bran and Luebbe segmented flow colorimetric autoanalyser using classical analytical techniques as described in Woodward and Rees (2001). Water samples were collected directly from the Niskin bottles at each station. Clean sampling and handling techniques were employed, and where possible were carried out according to the International GO-SHIP recommendations (Hydes et al., 2010). Nutrient reference materials (KANSO Japan) were run each day to check analyser performance and to guarantee the quality of the final reported data. The typical uncertainty of the analytical results was between 2 and 3%, and the limits of detection were 0.02 μmoles L^{-1} for nitrate + nitrite and phosphate. All samples were analysed within 1–2 h of sampling. Nutrient data are presented in Humphreys et al. (this issue).

Samples for total Chl-*a* were collected by filtering 200–250 mL of sea water through 25 mm diameter Fisherbrand MF300 or Whatman GF/F filters (effective pore size 0.7 μm). After filtration, pigments were extracted in 90% acetone for 18–20 h in the dark at 4 °C. Chlorophyll *a* concentration was determined fluorometrically on a Turner Trilogy fluorometer using a non-acidification module and calibrated with a

pure chlorophyll-*a* standard (Sigma-301 Aldrich, UK). Instrument drift was monitored and adjusted for using a solid-secondary standard (Turner Designs).

Daily rates of particulate gross primary production were scaled up from short-term (6–8 h, dawn to midday) rates of carbon fixation to seasonally adjusted day lengths (14 h in April). Rates of dissolved organic carbon production (*p*DOC) were determined at three depths (60%, 20% and 1% of surface irradiance) from the same bottles and incubations as for carbon fixation using methods adapted from López-Sandoval et al. (2011) and Poulton et al. (2016). It is expected that the daily rates of primary production presented in this paper based on short-term (< 8 h) incubations, better approximate 'gross primary production', whilst daily rates presented in companion papers (Mayers et al., this issue; Poulton et al., this issue), based on long-term (24 h) incubations better approximate 'net primary production' (see e.g. Marra, 2002).

For carbon fixation and *p*DOC, water samples were collected into four 70 mL polycarbonate bottles (3 light, 1 dark), and spiked with 6–11 μCi carbon14 (^{14}C) labelled sodium bicarbonate. The bottles were then incubated in a purpose-built constant temperature containerised laboratory at a range of seasonally adjusted irradiance levels (daily photon fluxes) using LED light panels and neutral density filters. Daylight LED light panels (Powerpax, UK) provided 100 μmol photons $m^{-2} s^{-1}$. Daily light doses were: 22.2, 13.1, 6.0, 3.4, 1.1 and 0.4 mol quanta $m^{-2} d^{-1}$ (corresponding to 60, 40, 20, 10, 5 and 1% of surface irradiance). The average surface irradiance for the cruise was 33.9 mol quanta $m^{-2} d^{-1}$, range 18.1–45.4 mol quanta $m^{-2} d^{-1}$ (see Poulton et al., this issue). The incubation temperatures were within ± 1 °C of the in situ temperature. On termination of the incubation, 5 mL sub-samples were filtered through 25 mm 0.2 μm polycarbonate filters, with the filtrates transferred to 20 mL scintillation vials for *p*DOC estimates. To remove the dissolved inorganic ^{14}C, 100 μL of 50% HCl was added to each vial, which were then sealed with a gas-tight rubber septum (Kimble-Kontes) and a centre well (Kimble-Kontes) containing a CO_2 trap (Whatman GFA filter soaked with 200 μL β-phenylethylamine) (see Mayers et al., this issue). After 12 h, the CO_2 traps were removed and disposed of, and 15 mL of Ultima Gold (Perkin Elmer, UK) liquid scintillation cocktail was added to the filtrate. Spike activity was checked following Mayers et al. (this issue) and activity in the filtrates was determined in a Tri-Carb 3100TR Liquid Scintillation Counter.

The remainder of each sample was then filtered through 25 mm 0.4 μm polycarbonate filters (Nuclepore™, USA), with extensive rinsing to remove any unfixed ^{14}C-labelled sodium bicarbonate, and 12 mL of Ultima Gold (Perkin-Elmer, UK) liquid scintillation cocktail added. The activity on the filters was then determined using a Tri-Carb 3100TR Liquid Scintillation Counter on-board. The average coefficient of variation was 9% (range < 1–74%, with higher coefficients of variation associated with low rates at the base of the euphotic zone).

2.3. Bacterial abundance

Samples for the enumeration of bacteria were collected from the Niskin bottles into clean 250 mL polycarbonate bottles. Subsamples were then pipetted into 2 mL microcentrifuge tubes and fixed with glutaraldehyde (50%, TEM grade, 0.5% final concentration) within 30 min of collection. After fixing for 30 min at 4 °C, samples were stained with SYBR Green I DNA dye (Invitrogen) for 1 h at room temperature in the dark and then analysed by flow cytometry (Tarran et al., 2006). The mean coefficient of variation for the flow cytometric analysis of bacterial abundance (BA) following this protocol was 2.3%, based on the means and standard deviations of 160 sets of duplicate and triplicate bacterial abundance analyses from Station L4 of the Western English Channel Observatory, Plymouth, UK.

2.4. Respiration derived from dissolved oxygen consumption

Five of the 6 light depths detailed above (60, 40 or 20, 10, 5 and 1% of surface irradiance) and the sample depth below the euphotic zone, were sampled for plankton community respiration (CR_{O2}). CR_{O2} was determined by measuring the decrease in dissolved oxygen after a 24 h incubation in the dark. Dissolved oxygen concentration was measured by automated Winkler titration performed with a Metrohm 765 burette to a photometric end point (Carritt and Carpenter, 1966). Ten gravimetrically calibrated 60 mL borosilicate glass bottles were carefully filled with seawater from each 10 L carboy. Water was allowed to overflow during the filling, and care was taken to prevent air bubble formation in the silicone tube. Five bottles were fixed at the start of the incubation ("zero") with 0.5 mL of 3 M manganese sulphate and 0.5 mL of 4 M sodium iodide/8 M sodium hydroxide solution (Carritt and Carpenter, 1966). The remaining five bottles were placed underwater in darkened temperature controlled incubators located in a temperature controlled room for 24 h ("dark"). The incubation temperatures were within ± 0.5 °C of the in situ temperature. "Dark" bottles were fixed as described for the "zero" bottles after 24 h. Daily plankton community respiration was calculated from the difference in oxygen concentration between the mean of the replicate "zero" measurements and the mean of the replicate "dark" measurements, assuming a linear decrease over 24 h. The standard error (± SE) of the net change was calculated as the square root of the sum of the squares of the SEs of the "zero" and "dark" replicates.

The average percentage coefficient of variation was 0.15% for both the "zero" and "dark" replicate oxygen concentrations (n = 36 in each case).

2.5. Respiration derived from INT reduction

Five 200 mL dark glass bottles were filled with seawater from each 10 L carboy. Two replicates were immediately fixed by adding formaldehyde (2% w/v final concentration) and used as controls. All five bottles were then inoculated with a sterile solution of 7.9 mM 2-(ρ-iodophenyl)-3-(ρ-nitrophenyl)-5phenyl tetrazolium chloride (INT) to give a final concentration of 0.8 mM. The solution was freshly prepared for each experiment using Milli-Q water. Samples (+ controls) were incubated in the same temperature-controlled water bath as the dissolved oxygen bottles for 0.5–0.8 h. Incubations were terminated by adding formaldehyde to the three replicates, as done previously for the controls. Each sample and control were then filtered through 0.8 μm and onto 0.2 μm pore size polycarbonate filters, and the filters were air-dried, and stored frozen. The INT reduced in each size fraction (i.e. > 0.8 μm and 0.2–0.8 μm) was extracted with propanol and the absorbance at 485 nm determined using a Beckman model DU640 spectrophotometer following Martínez-García et al. (2009). The INT reduced was calculated as the average INT reduced in the three incubated samples minus the average of the INT reduced in the two controls for each size fraction. Thus, the measurements are corrected for any interference by the absorbance of the water due to turbidity or reduction of INT caused by non-metabolic factors (i.e. organic matter content). The rate measured in the large size-fraction ($INT_{>0.8}$) will result mainly from INT reduction by eukaryotes and particle-attached bacteria. Since the combined abundance of *Synechococcus* and *Prochlorococcus* made up only 1% of the total abundance of *Synechococcus*, *Prochlorococcus* and bacteria (data not shown), the main respiring organisms in the small size-fraction ($INT_{0.2–0.8}$) are expected to be free living heterotrophic bacteria. The total plankton community respiration (INT_T) in μmol $INT_f L^{-1} h^{-1}$ is calculated as the sum of the INT reduction in the two size fractions ($INT_{0.2–0.8}$ and $INT_{>0.8}$).

A time-course experiment was carried out on water collected from 5 m on the 4th of April 2015 in order to determine the optimal incubation time for INT reduction. The maximum incubation time before the INT became toxic for the plankton community (and so the rate of

Table 1
Characterization of the central Celtic Sea (CCS) sampling station: euphotic depth (depth of 1% surface irradiance), depth of the pycnocline, surface temperature, and range of nitrate + nitrite and phosphate concentrations in the euphotic zone.

Sampling day	Depth 1% I_0 (m)	Depth pycnocline (m)	Temperature (°C)	Nitrate + nitrite (μM)	Phosphate (μM)
04/04/2015	37	51	9.9	6–6.1	0.5
06/04/2015	37	47	9.9	5.6–5.7	0.4–0.5
11/04/2015	32	30	10.3	3.8–4.9	0.3–0.4
15/04/2015	28	15	10.7	1.3–4.1	0.2–0.4
20/04/2015	28	30	10.6	2–2.9	0.2–0.3
25/04/2015	35	16	11.1	0.4–2.8	0.1–0.2

INT reduction began to decrease) was 1 h and hence all our incubations were undertaken for 0.5–0.8 h. The INT reduction technique, which includes a post-incubation filtration and an incubation < 1 h, allows the determination of more realistic rates of bacterial respiration than the traditional 0.8 μm pre-filtered 24 h bottle incubation technique (Aranguren-Gassis et al., 2012). INT reduction was converted into units of oxygen consumption by applying the equation Log O_2 = 0.80Log INT_T + 0.45 (R^2 = 0.43, p < .0001, n = 97) derived from the comparison of the 97 concurrent measurements of CR_{O2} and INT_T rates measured during November 2014, April and July 2015 (see Garcia-Martin et al., this issue and Supplementary Fig. 1).

Plankton and bacterial respiration in units of O_2 consumption were then converted into units of carbon production using a constant respiratory quotient of 1 (Buchanan et al., 2000; Williams and del Giorgio, 2005). We are aware that plankton and bacterial respiratory quotients are not constant and vary according to the composition of the substrate being oxidized (Berggren et al., 2012; Robinson and Williams, 1999; Williams and del Giorgio, 2005). However, without any information on substrate composition we have to assume a constant value and accept an error associated with this conversion of ~20%.

2.6. Heterotrophic bacterial production and bacterial growth efficiency

Bacterial production (BP) was calculated from ^{14}C leucine incorporation using a theoretical approach assuming no isotope dilution (Kirchman, 2001). Water samples (125 mL) were collected from the same 6 Niskin bottles as those sampled for plankton respiration detailed above, into acid-washed polycarbonate bottles. Aliquots of 10 μL ^{14}C leucine working solution (0.04 MBq mL^{-1}) were pipetted into 2 mL sterile centrifuge tubes with 1.6 mL of sample water and mixed.

For each depth two replicates were incubated for 0, 1, 2 and 3 h in the dark at in situ temperatures. Samples were fixed with 80 μL of 20% paraformaldehyde (final concentration of 1%) and filtered onto 0.2 μm polycarbonate filters (pre-soaked in 1 mM non-labelled leucine). Sample vials were washed with deionised water to rinse any remaining label from each vial. Then filters were inserted into scintillation vials, dried overnight at room temperature and mixed with 4 mL of Optiphase Hi-Safe II scintillation fluid. Radioactivity in the samples was measured using a Beckman Coulter LS6500 liquid scintillation counter with the efficiency of counting determined using the external quench monitor method. [^{14}C]leucine incorporation was calculated from counts (corrected for quenching) according to Kirchman (2001) using isotope specific activity values corrected for decay (Stewart and Hawcroft, 1977). Bacterial production was derived from the slope of a regression of the disintegrations per minute at the 4 incubation times. The precision of the technique ranged from 0.0003 to 0.0112 with a median value of 0.0027 μg C L^{-1} d^{-1}.

Cell-specific bacterial production and respiration were calculated by dividing BP and $INT_{0.2–0.8}$ by BA, respectively. Bacterial carbon demand (BCD) was calculated as: BCD = BP + $INT_{0.2–0.8}$ and bacterial growth efficiency (BGE) as: BP/BCD.

2.7. Data analysis

Euphotic depth integrated CR_{O2}, INT_T, $INT_{0.2–0.8}$, PP and BP rates were calculated by trapezoidal integration of the volumetric rates measured at the five depths within the euphotic depth. The standard errors (± SE) of the integrated rates were calculated following the propagation procedure for independent measurements described by Miller and Miller (1988). The depth-integrated contribution of the 0.2–0.8 μm fraction to total plankton community respiration (% $INT_{0.2–0.8}$) was calculated as the depth-integrated $INT_{0.2–0.8}$ divided by the depth-integrated INT_T and multiplied by 100.

Statistical analyses were performed with SPSS software. Spearman non-parametric correlation tests were used to study the relationship between volumetric CR_{O2}, INT_T, $INT_{0.2–0.8}$, PP and BP and between each of these and other physicochemical and biological parameters (temperature, nitrate + nitrite and phosphate concentration, Chl-*a* concentration, bacterial abundance).

Fig. 2 was produced with Ocean Data View (ODV) software (Schlitzer, 2015).

3. Results

3.1. Hydrographic and nutrient conditions

A full description of the hydrographic and nutrient conditions present at CCS between 4th April and 25th April 2015 is presented in Wihsgott et al. (this issue) and Humphreys et al. (this issue) and a brief overview is given in Table 1. The water column was stratified with a pycnocline at 51–47 m at the beginning of the sampling period (4th and 6th April) (Fig. 2) with colder and less saline waters at the surface. The depth of the euphotic zone decreased after the 6th of April when the pycnocline also shoaled to less than 47 m (Table 1). Nutrient concentrations were vertically homogenous in the water column during the first two sampling days (4th and 6th April) with high concentrations of nitrate + nitrite and phosphate (~6 ± 0.07 μmol L^{-1} and ~0.5 ± 0.01 μmol L^{-1}, respectively) (Humphreys et al., this issue).

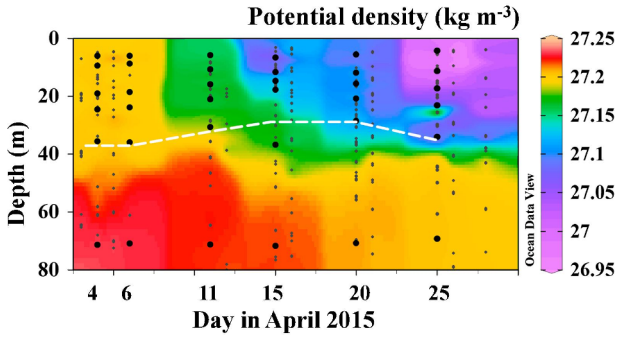

Fig. 2. Potential density during April 2015 at the CCS station. Smaller black dots represent the CTD data used to derive the contour plot (n = 40 vertical profiles), larger black dots show the depths where water samples were collected and the white dotted line is the euphotic depth (1% surface irradiance).

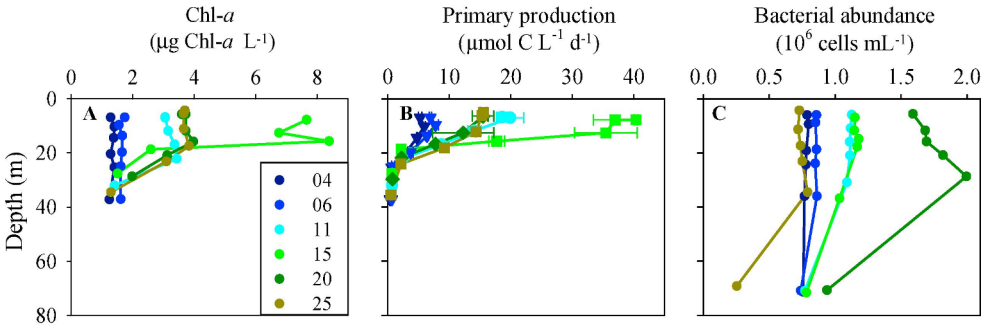

Fig. 3. Vertical profiles of (A) chlorophyll-*a* concentration (µg Chl-*a* L^{-1}), (B) primary production (µmol C L^{-1} d^{-1}) and (C) bacterial abundance (10^6 cells mL^{-1}) during April 2015.

Nutrient concentrations decreased above the pycnocline over the following 15 days to a nitrate + nitrite concentration of 0.4–0.7 µmol L^{-1} and a phosphate concentration between 0.13 and 0.15 µmol L^{-1} on the 25th April. Nutrients remained high below the pycnocline, in the aphotic zone, and a marked nitracline developed at ~20 m.

3.2. Total chlorophyll-a and primary production

Chlorophyll-*a* vertical profiles showed a well-mixed distribution during 4th and 6th April (Fig. 3A). After this time, the vertical distribution of Chl-*a* was characterised by higher (sub-) surface (5–16 m) values and a progressive decrease with depth. Maximum values were recorded on the 15th of April with surface values of 7.7 µg Chl-*a* L^{-1} and a maximum Chl-*a* of 8.4 µg Chl-*a* L^{-1} at 16 m. Chl-*a* concentrations decreased sharply between the 15th and 20th April, and measured 3.7 µg Chl-*a* L^{-1} on the 25th April. Chl-*a* values at the base of the euphotic layer were similar throughout the sampling period (< 2 µg Chl-*a* L^{-1}).

Primary production profiles showed a similar temporal pattern to Chl-*a* with low rates in surface waters on the first two days (< 8 µmol C L^{-1} d^{-1}) increasing to 19.9 µmol C L^{-1} d^{-1} on the 11th April and reaching maximum values on the 15th April (~40 µmol C L^{-1} d^{-1}) (Fig. 3B). Primary production had decreased by the 20th April to similar values as on the 11th of April and remained at these rates until the 25th April (Fig. 3B).

Euphotic zone depth-integrated gross primary production increased > 5-fold between the 4th and the 15th of April, decreased by ~50% between the 15th and the 20th of April and then remained relatively stable until the 25th of April (Table 2).

3.3. Bacterial abundance

Bacterial abundance followed a similar temporal trend to Chl-*a* with a homogenous vertical distribution during the first two days ranging from 0.75 to 0.86 10^6 cells mL^{-1} (Fig. 3C). On the 11th April, when the euphotic depth became shallower, bacterial abundance increased to > $1.2 \cdot 10^6$ cells mL^{-1} (Fig. 3C). However, whereas the peak in Chl-*a* occurred on the 15th April, the highest bacterial abundance occurred on the 20th April ($1.9 \cdot 10^6$ cells mL^{-1}). Bacterial abundance decreased again by the 25th April ($0.74 \cdot 10^6$ cells mL^{-1}) to values similar to those at the beginning of the sampling period ($0.79 \cdot 10^6$ cells mL^{-1}). There was no distinct increase in bacterial abundance in the aphotic zone, with values remaining around $0.7–0.9 \cdot 10^6$ cells mL^{-1} for the period from the 4th to 20th April, decreasing to $0.2 \cdot 10^6$ cells mL^{-1} on the 25th April.

3.4. Plankton and bacterial metabolism

There was a significant correlation between oxygen consumption (µmol O_2 L^{-1} d^{-1}) and INT reduction (µmol INT_f L^{-1} h^{-1}) measured during April 2015 ($r = 0.78$, $p < .0001$, $n = 32$, Supplementary Figs. 1 and 2), confirming the validity of the INT_T technique as a proxy for plankton respiration and endorsing the conversion of INT reduction into units of oxygen consumption (Fig. 4A).

Plankton community respiration (CR_{O2}) at ~10 m increased from < 1.4 ± 0.49 µmol O_2 L^{-1} d^{-1} before the strengthening of the pycnocline (4th and 6th April) to 8.05 ± 0.58 µmol O_2 L^{-1} d^{-1} on the day of highest Chl-*a* (15th April) (Fig. 4B). CR_{O2} decreased to < 4.00 ± 0.25 µmol O_2 L^{-1} d^{-1} by the 20th April, and increased again by the 25th. CR_{O2} in the aphotic zone varied relatively little between the sampling days (0.35 ± 0.14–1.22 ± 0.55 µmol O_2 L^{-1} d^{-1}). Changes in plankton respiration were mainly driven by changes in the respiration of the > 0.8 µm size fraction (Fig. 4C).

Euphotic depth-integrated rates of CR_{O2} increased 5.4-fold from the 4th of April to the 15th of April (Table 2) when the respiration maximum occurred in sub-surface waters (10–20 m), and then decreased on the 20th of April at the same time as a decrease in depth-integrated PP. The maximum depth-integrated respiration rate was observed on the 25th of April due to the high respiration rates measured below 20 m.

There was a significant relationship between PP and CR_{O2} for the first 5 days ($r = 0.9$, $p = .037$, $n = 5$) of the study, but not for the duration of the study ($r = 0.71$, $p = .11$, $n = 6$), indicating a co-evolution of the two variables during the pre-bloom and bloom period (4–20th April), but not in the late post-bloom (25th April) when the highest depth-integrated plankton respiration rate was measured while PP had intermediate values (Table 2 and Supplementary Fig. 3). The euphotic zone was net autotrophic (PP > CR_{O2}) during the whole sampling period with maximum values of PP-CR_{O2} on the 15th April

Table 2
Euphotic depth-integrated chlorophyll-*a* concentrations (Chl-*a*), daily plankton community respiration (CR_{O2}), bacterial respiration ($INT_{0.2–0.8}$), percentage of bacterial respiration (% $INT_{0.2–0.8}$), bacterial production (BP), gross primary production (PP) and the balance between primary production and plankton respiration (PP - CR_{O2}) measured during April 2015 (± SE, except for PP which is ± SD). nd denotes no data. Chl-*a* values are presented in Hickman et al. (this issue).

Sampling Day	Chl-*a* mg Chl-*a* m^{-2}	CR_{O2} mmol O_2 m^{-2} d^{-1}	$INT_{0.2–0.8}$ mmol O_2 m^{-2} d^{-1}	% $INT_{0.2–0.8}$ %	BP mg C m^{-2} d^{-1}	PP mmol C m^{-2} d^{-1}	PP - CR_{O2} mmol C m^{-2} d^{-1}
04/04/2015	49.6	22 ± 3.6	16.0 ± 2.9	37.4 ± 9.8	48.2 ± 2.7	114.5 ± 4.6	92.5 ± 5.8
06/04/2015	61.4	47.5 ± 4.9	nd	nd	52.7 ± 1.8	148.2 ± 7.4	100.7 ± 8.9
11/04/2015	94.9	77.2 ± 4	8.2 ± 1.5	13.2 ± 2.6	112.1 ± 4.3	314.3 ± 16	237.1 ± 23.3
15/04/2015	152.6	119.2 ± 3.6	13.7 ± 1.9	15.9 ± 2.4	118.2 ± 4.7	613 ± 27.7	493.8 ± 27.9
20/04/2015	96.6	84.8 ± 3.3	10.4 ± 1.3	12.3 ± 1.6	132.7 ± 7.3	264.2 ± 38.2	179.4 ± 33.1
25/04/2015	109.2	147 ± 4.2	10.8 ± 0.6	16.3 ± 1.2	128.7 ± 3.0	304.1 ± 9.9	157.1 ± 10.7

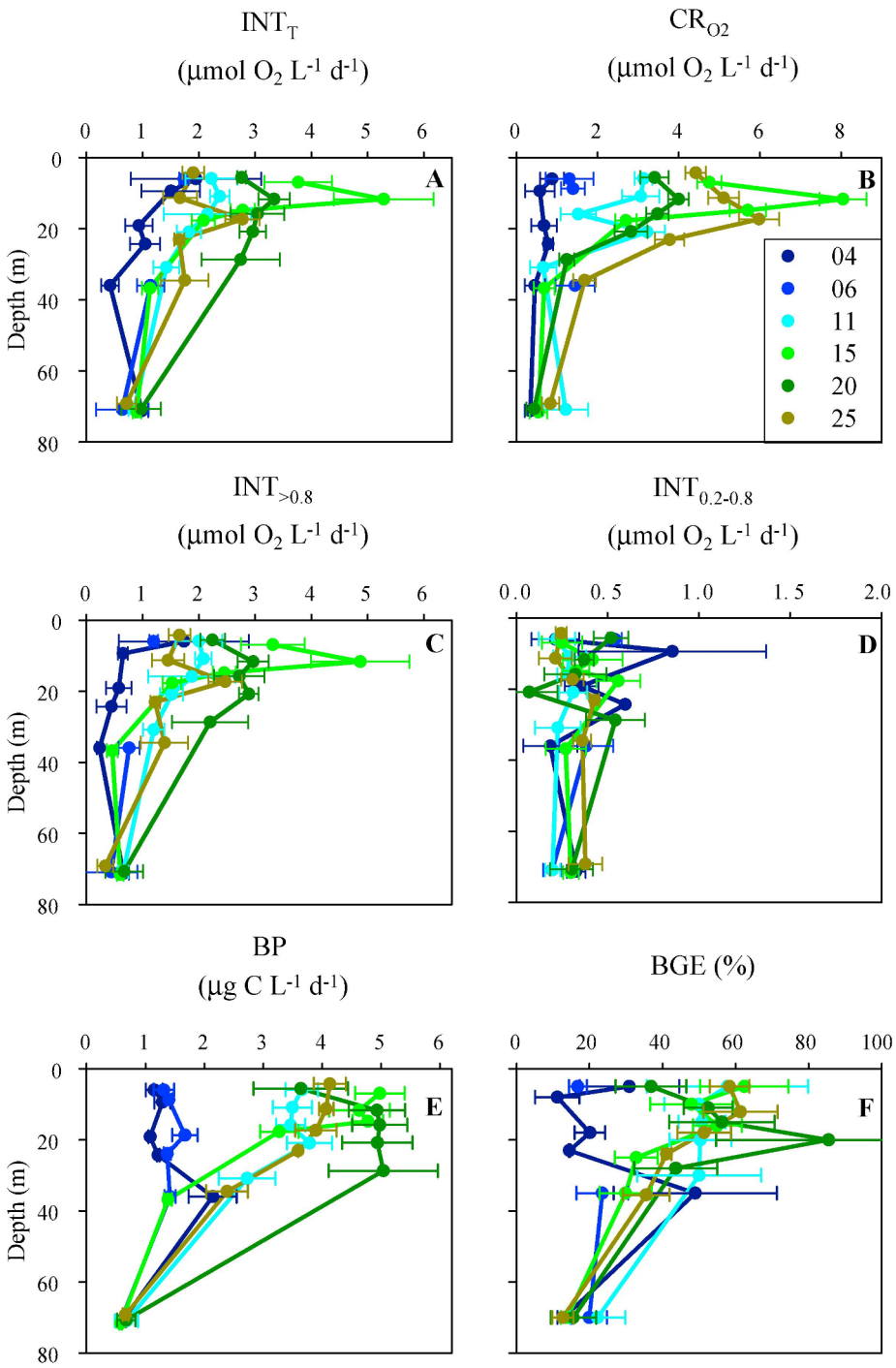

Fig. 4. Vertical profiles of (A) plankton community respiration (INT_T), (B) plankton community respiration (CR_{O2}), (C) respiration of the plankton fraction > 0.8 µm ($INT_{>0.8}$), (D) bacterial respiration ($INT_{0.2–0.8}$), (E) bacterial production (BP) and (F) bacterial growth efficiency (BGE) during April 2015. Error bars represent the standard error between sample bottles.

(490 mmol C m^{-2} d^{-1}) (Table 2).

Free-living bacterial respiration ($INT_{0.2–0.8}$) was less variable over time than plankton community respiration, and did not vary significantly with depth (Fig. 4D). Euphotic depth-integrated bacterial respiration was 16.0 ± 2.9 mmol O_2 m^{-2} d^{-1} on the 4th April, decreasing to 8.2 ± 1.5 mmol O_2 m^{-2} d^{-1} on the 11th April, and remained fairly constant until the 25th April (Table 2).

The proportion of plankton community respiration attributable to free-living bacteria (%$INT_{0.2–0.8}$) was 37 ± 10% at the beginning of the sampling period (4th and 6th April) decreasing to around 16 ± 3% on 15th April (Table 2). The decrease in%$INT_{0.2–0.8}$ was due to an increase in $INT_{>0.8}$.

Bacterial production in the upper 20 m increased from ~1 µg C L^{-1} d^{-1} on the 4th and 6th April to a maximum of 3–5 µg C L^{-1} d^{-1}) on the 20th April (Fig. 4E). There was no difference in the rates of BP on the 15th and 20th of April in the upper 18 m but there was a 1.5- to 4-fold increase in rates in waters deeper in the euphotic zone. Bacterial production in the aphotic zone remained consistently low between 0.59 ± 0.01 and 0.68 ± 0.20 µg C L^{-1} d^{-1}. In contrast to bacterial respiration, euphotic depth-integrated bacterial production rates increased 2.3-fold before the Chl-*a* maximum on 15th April, and 2.8-fold by the maximum in bacterial abundance on the 20th April (Table 2) which was 5 days after the maxima in Chl-*a*, PP, CR_{O2} and INT_T. The low bacterial numbers measured on the 25th April (Fig. 3C) were associated with high bacterial production, suggesting greater metabolic efficiency. Bacterial production was significantly

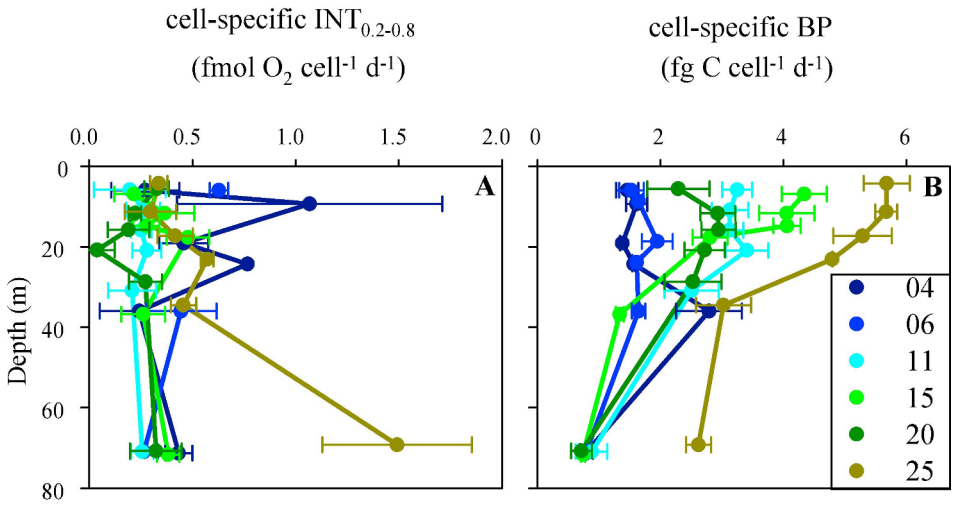

Fig. 5. Vertical profiles of cell-specific bacterial respiration (A) and bacterial production (B) during April 2015. Error bars represent the standard error of the measurements.

correlated to PP (r = 0.51, p = .004, n = 30), with PP able to explain 28% of the variability in BP.

Cell-specific bacterial metabolism showed different trends for bacterial respiration and production. There was no significant difference between cell-specific bacterial respiration between days ($p > .5$, t-test) (Fig. 5A). However, cell-specific bacterial production increased gradually during the development of the phytoplankton bloom (from 1.4 fg C cell^{-1} d^{-1} to 5.7 fg C cell^{-1} d^{-1}) with maximum cell-specific production rates on 25th April as a consequence of the lower bacterial abundance (Fig. 5B).

In order to get an indication of whether the local primary production could support the bacterial carbon demand, the depth-integrated organic matter production (particulate and dissolved) minus the autotrophic losses (considered as the INT$_{>0.8}$) was compared with the bacterial carbon demand (BCD). Depth-integrated BCD ranged between 2.4 and 6.5% of the depth integrated organic matter available (Fig. 6), indicating that the organic carbon produced by phytoplankton was between 20 and 40 times greater than the carbon requirements of the bacteria.

Bacterial growth efficiencies (BGE) were lowest (high bacterial respiration associated with low bacterial production) at the beginning of the spring bloom (< 31%) and increased on the 11th April to 40–60%, remaining at this level until the 25th April (Fig. 4F). In general, the greater variability in bacterial production was reflected in the variability in BGEs (Fig. 7A and B) which were always higher in the euphotic zone than in the aphotic zone (range 13–22%).

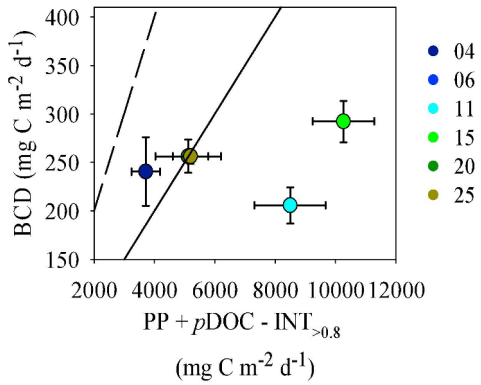

Fig. 6. Relationship between the bacterial carbon demand (BCD) and the locally produced organic carbon available for the bacteria, considered as the sum of particulate organic carbon (PP) and dissolved organic carbon production (*p*DOC) minus the respiration of the autotrophic plankton (INT$_{>0.8}$). Lines represent when the BCD: (PP + *p*DOC − INT$_{>0.8}$) ratio equals 5 (solid line) and 10% (dashed line).

4. Discussion

April 2015 in the central Celtic Sea was characterised by a reduction in vertical mixing and the formation of a well-stratified upper layer, typical for the spring period in shelf seas (Pingree et al., 1976; Fasham et al., 1983). The change in the water column structure allowed the initiation of a spring bloom (Henson et al., 2006; Wihsgott et al., this issue), seen as a sharp increase in Chl-*a* concentration, which lasted less than 15 days (Fig. 3A). This brief but intense increase in Chl-*a* is typical of spring-blooms in these temperate waters (Joint et al., 2001; Fileman et al., 2011). In ten days, depth-integrated Chl-*a* concentrations increased 3-fold in the euphotic zone associated with a 5-fold increase in both gross primary production and plankton community respiration (Table 2). The range in magnitude of primary production was greater than the range in respiration in the euphotic layer (Table 2) during the spring bloom period. There was a clear temporal trend in the balance between gross primary production and respiration (PP – CR_{O2}) increasing from the pre-bloom period to a maximum on 15th of April alongside the maximum in Chl-*a*. There was a decrease in the PP – CR_{O2} balance after the bloom but it always remained positive. The higher production compared to respiration indicates a high concentration of particulate organic matter available for export to deeper waters or transfer to higher trophic levels. In fact, the concentrations of particulate organic carbon (POC) in the aphotic layers, below the pycnocline, significantly increased from 3 µmol L^{-1} on 15th April to 5 µmol L^{-1} on 20th April (Davis et al., this issue) suggesting that a proportion of the excess POC was exported from the surface layers to deeper waters.

Phytoplankton can quickly adjust the amount of cellular pigments, antennae and reception points to increase the efficiency of photosynthesis (Falkowski and Owens, 1980; Moore et al., 2006) when nutrients and light are available. The restructuring of the photosynthetic apparatus and the synthesis of new reaction centres are associated with a higher energetic demand (Falkowski and Raven, 2007), and presumably a higher rate of phytoplankton respiration. This is consistent with our results and the fact that plankton community respiration rates, and in particular the respiration associated with the size class > 0.8 µm, increased in parallel with the increases in the abundance of autotrophic dinoflagellates and ciliates (Tarran et al., this issue) and gross primary production (Table 2) during the spring bloom (see also Mayers et al., this issue; Poulton et al., this issue). Previous studies of spring phytoplankton blooms based on a sampling interval of ca. 5–15 days also observed an increase in plankton community respiration rates associated with an increase in production (Blight et al., 1995; Caffrey et al., 1998) but with a time lag of ≤1 week (Caffrey et al., 1998) to a fortnight (Blight et al., 1995). The higher sampling frequency in our study (2–5 days) than in the former studies allowed us to observe the parallel

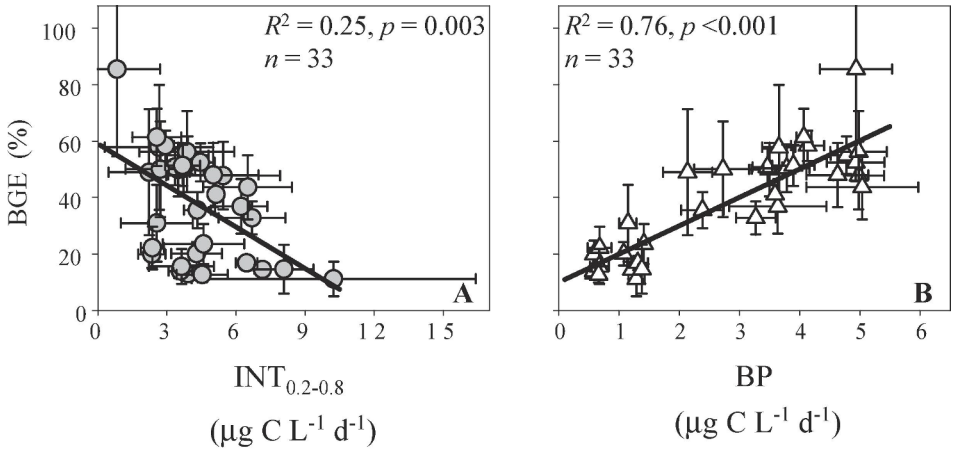

Fig. 7. Relationship between: (A) bacterial respiration ($INT_{0.2–0.8}$) and (B) bacterial production (BP) and bacterial growth efficiency (BGE) throughout the water column. Error bars represent the standard error of the measurements and the solid lines the corresponding linear regression with R^2 the coefficient of determination, p the level of significance and n the number of data.

increase in PP and CR_{O2}. This parallel evolution would have been missed if our sampling frequency were reduced. For example if we only consider data from the 4th, 15th and 25th of April, we would have inferred a continuous increase in CR_{O2} with a maximum 10 days after the maximum in PP. However, when our data from 6th, 11th and 20th are included, the concurrent patterns of increase and decrease in both CR_{O2} and PP are revealed.

The occurrence or lack of a time lag between PP and CR_{O2} may be related to the plankton community structure and the capacity of the plankton to react rapidly to an increase in resources. In our study, nanophytoplankton (2–20 µm) dominated the bloom, both in terms of cell abundance (Tarran et al., this issue), Chl-*a* and primary production (Hickman et al., this issue), rather than the larger diatom and dinoflagellate taxa often considered to be typical of spring blooms in this area (Rees et al., 1999; Widdicombe et al., 2010; Van Oostende et al., 2012). Plankton communities dominated by small and fast growing cells are characterised by greater interactions between species and faster organic matter and energy cycling (Legendre and Le Fèvre, 1995; D'alelio et al., 2016) which could also contribute to the lack of a time lag between the increase in production and respiration.

Blight et al. (1995) suggested that the time lag they observed was due to the organic matter produced during a spring bloom only stimulating bacterial respiration a few days later. However, this is not consistent with our results, where bacterial abundance and production increased at the same time as the increase in Chl-*a*, reaching maxima on 20th April, 5 days after the maxima of Chl-*a*, primary production and respiration of the plankton fraction > 0.8 µm ($INT_{>0.8}$). The earlier maxima in primary production and plankton respiration compared to bacterial abundance could be related to a grazing effect. Nanophytoplankton are known to be active grazers on bacteria (Sherr and Sherr, 1994) and could have controlled the bacterial abundance during the pre-bloom period. Then, the increase of organic matter (particulate and dissolved, data not shown) on the 15th April and the decrease in the > 0.8 µm plankton biomass (in terms of Chl-*a* and abundance, data not shown) observed on the 20th April may have released the grazing pressure and stimulated a change in the bacterial community composition (Smith et al., 1995; Azam, 1998; Tada et al., 2011; Landa et al., 2015). In fact, there was a 1.6-fold increase in the abundance of bacterial cells with high nucleic acid content on the 15th of April and a 2.8-fold increase on the 20th of April compared to their abundance on the 11th of April (Fig. 2, and see Tarran et al., this issue). As different bacteria have different metabolic efficiencies, the phylotypes forming the bacterial community at the end of April may have been rapidly growing bacteria with higher production rates (Pedler et al., 2014). In addition, bacterial respiration was highest at the beginning of the sampling period and then remained relatively constant during and up to 10 days after the Chl-*a* maximum. This relative stability in bacterial respiration might be caused by a bias in the sampling methodology as the respiration of particle attached bacteria is not included. However, this problem is inherent to all studies where bacterial respiration is measured as the respiration of a size-class of the plankton (e.g. Blight et al., 1995), and so it is unlikely to explain the differences between our study and previous ones (Blight et al., 1995).

Depth-integrated BCD only accounted for < 6.5% of the net organic matter locally produced (production minus the autotrophic respiration), and this ratio was lowest at the peak of the bloom (2.5%) when primary production (particulate and dissolved) was highest. These estimates are lower than the bacterial carbon demands of 16–36% of primary production previously determined in the western north Atlantic during spring (Li et al., 1993). The low ratio in the Celtic Sea indicates that a large proportion (i.e. > 83%) of the phytoplankton-produced organic carbon was available for export to depth or for consumption by micro- and meso-zooplankton.

Changes in BP, and not in $INT_{0.2–0.8}$, influenced the changes in the BGEs observed during spring, which ranged from < 31% at the beginning of April when BP was low to 40–60% on 20th and 25th April when BP rates were highest. These results are in agreement with the high variability in BGE observed in natural waters (Del Giorgio and Cole, 1998; Robinson, 2008; Sintes et al., 2010; Guillemette et al., 2016) and can only be explained by an uncoupling of bacterial production and respiration or a shift in the bacterial community structure to predominantly cells with high growth efficiencies (Del Giorgio and Gasol, 2008) at the end of the sampling period. The uncoupling could occur through a shift in the bacterial activity from using carbon resources for cell maintenance at the beginning of April to biomass production at the end of April. A recent study of bacterial metabolism in Canadian freshwater lakes showed how bacteria preferred dissolved organic carbon (DOC) from algal sources over that from terrestrial sources (Guillemette et al., 2016). In addition, this study demonstrated how bacteria allocated the DOC to either biomass production or respiration depending on its origin, with more algal DOC being channelled to respiration. Our measurements do not allow us to determine the allocation of organic carbon to bacterial biomass or respiration, but the increase in primary production, phytoplankton-produced dissolved organic carbon and the subsequent increase in bacterial production but not bacterial respiration does indicate different pathways for the carbon.

Importantly, our results suggest that calculations of marine carbon budgets should take into account the high variability in BGE observed. This is in direct contrast to previous assumptions of a constant BGE (for example, of 50% in the Celtic Sea study of Joint et al., 2001). Our average BGE of 39 ± 3% was higher than the average of 20% reported for many marine systems (Del Giorgio and Cole, 1998) but is within the range of BGEs measured in the North Sea during spring (16–39%, Reinthaler and Herndl, 2005 and 18–43%, Sintes et al., 2010) and in temperate upwelling-induced phytoplankton blooms (34 ± 5–52 ± 7% Teira et al., 2015

and 17–62%, Wear et al., 2015). In common with all other direct determinations of BGE, the BGEs presented here include the bias that while estimates of BP include the production of particle attached bacteria, estimates of the respiration of a bacterial size fraction of the plankton do not.

BGEs are affected by temperature (Rivkin and Legendre, 2001), inorganic nutrient availability (Rivkin and Anderson, 1997; Lønborg et al., 2011) and the quality of the available dissolved organic matter (Goldman et al., 1987; Lemée et al., 2002; Reinthaler and Herndl, 2005). We observed a positive correlation between BGE and temperature despite the small range in temperature (9.9–11.1 °C) which occurred during our study. The inverse covariation between nitrate + nitrite and PP, and the positive correlation between BGE and PP contributed to the negative correlation between BGE and inorganic nitrate + nitrite ($r = -0.77$, $p < .0001$, $n = 33$), contrary to the analysis by Lønborg et al. (2011). The increase in BGE and in BP may have been driven by a change in the quality of the available dissolved organic material (Benner et al., 1995; Jiao et al., 2014), as the DOC:DON ratio decreased slightly from 25 ± 4 on the 4th April to 17 ± 3 on the 25th April (Davis et al., this issue). Unfortunately, there are only three days when both DOM composition and bacterial metabolism were measured, precluding any statistical analysis.

In summary, the strong covariation in the rates of primary production and plankton community respiration during the spring bloom implies that the same physicochemical conditions that stimulated PP also enhanced CR_{O2}. There was no 4–5 day time lag between PP and CR_{O2} in contrast to previous studies of diatom-dominated blooms. The increase in CR_{O2} was driven by an increase in respiration of the > 0.8 μm size fraction (presumably phytoplankton and heterotrophic eukaryotes) rather than in free-living bacterial respiration (0.2–0.8 μm size fraction). There was an increase in bacterial production while bacterial respiration was fairly constant throughout the phytoplankton bloom. Changes in bacterial growth efficiencies were driven by changes in bacterial production with values increasing from < 31% at the start of the phytoplankton bloom to 40–60% at the end of the bloom, suggesting that carbon budgets which rely on a constant BGE could be biased.

Acknowledgements

We thank the captain and crew of the *RRS Discovery* during DY029 cruise for their help and support at sea and all the scientists involved in the cruise. We would also like to thank Joanne Hopkins and Charlotte Williams (National Oceanographic Centre, Liverpool) for assistance and provision of the physical characterization of the area, E. Malcolm S. Woodward for the nutrient data and Clare E. Davis and Claire Mahaffey for the elemental characterization of the dissolved and particulate organic matter. This study is a contribution to the UK Natural Environment Research Council (NERC) Shelf Sea Biogeochemistry programme. E.EG-M was funded by NERC grant NE/K00168X/1 (awarded to C. Robinson and D. Purdie) and by a research grant from The Leverhulme Trust (RPG-2017-089 awarded to UEA) during the writing of this paper. SM, EM & CW were funded by NERC grant NE/K001884/1 (awarded to K. Davidson). We thank Ray Leakey for advice with bacterial production methodology and data. GT was funded by NERC grant NE/K002058/1. KM, AJP and CJD were funded by NERC grant NE/K001701/1 (awarded to A. Poulton).

Appendix A. Supplementary material

Supplementary data associated with this article can be found, in the online version, at http://dx.doi.org/10.1016/j.pocean.2017.11.002.

References

Amon, R.M.W., Benner, R., 1994. Rapid cycling of high-molecular-weight dissolved organic matter in the ocean. Nature 369, 549–552.

Amon, R.M.W., Benner, R., 1996. Bacterial utilization of different size classes of dissolved organic matter. Limnol. Oceanogr. 41, 41–51.

Aranguren-Gassis, M., Teira, E., Serret, P., Martínez-García, S., Fernández, E., 2012. Potential overestimation of bacterial respiration rates in oligotrophic plankton communities. Mar. Ecol. Prog. Ser. 453, 1–10.

Azam, F., 1998. Microbial control of oceanic carbon flux: the plot thickens. Science 280, 694–696.

Barnes, M.K., Tilstone, G.H., Suggett, D.J., Widdicombe, C.E., Bruun, J., Martinez-Vicente, V., Smyth, T.J., 2015. Temporal variability in total, micro-and nano-phytoplankton primary production at a coastal site in the western English Channel. Prog. Oceanogr. 137, 470–483.

Behrenfeld, M.J., 2010. Abandoning Sverdrup's critical depth hypothesis on phytoplankton blooms. Ecology 91, 977–989.

Benner, R., Opshal, S., Chin-Leo, G., 1995. Bacterial carbon metabolism in the Amazon River system. Limnol. Oceanogr. 40 (7), 1262–1270.

Berggren, M., Lapierre, J.-F., Del Giorgio, P.A., 2012. Magnitude and regulation of bacterioplankton respiratory quotient across freshwater environmental gradients. ISME J. 6, 984–993.

Biddanda, B., Benner, R., 1997. Carbon, nitrogen, and carbohydrate fluxes during the production of particulate and dissolved organic matter by marine phytoplankton. Limnol. Oceanogr. 42, 506–518.

Blight, S., Bentley, T., Lefevre, D., Robinson, C., Rodrigues, R., Rowlands, J., Williams, P.J. le B., 1995. Phasing of autotrophic and heterotrophic plankton metabolism in a temperate coastal ecosystem. Mar. Ecol. Prog. Ser. 128, 61–75.

Buchanan, B.B., Gruissem, W., Jones, R.L., 2000. Biochemistry and Molecular Biology of Plants. American Society of Plant Physiologists, Rockville, MD.

Caffrey, J.M., Cloern, J.E., Grenz, C., 1998. Changes in production and respiration during a spring phytoplankton bloom in San Francisco Bay, California, USA: implications for net ecosystem metabolism. Mar. Ecol. Prog. Ser. 172, 1–12.

Carritt, D.E., Carpenter, J.H., 1966. Comparison and evaluation of currently employed modifications of the Winkler method for determining dissolved oxygen in seawater; a NASCO Report. J. Mar. Res. 24, 286–319.

D'Alelio, D., Libralato, S., Wyatt, T., D'Alcalà, M.R., 2016. Ecological-network models link diversity, structure and function in the plankton food-web. Sci. Rep. 6, 21806. http://dx.doi.org/10.1038/srep21806.

Danger, M., Oumarou, C., Benest, D., Lacroix, G., 2007. Bacteria can control stoichiometry and nutrient limitation of phytoplankton. Funct. Ecol. 21, 202–210.

Daniels, C.J., Poulton, A.J., Esposito, M., Paulsen, M.L., Bellerby, R., St. John, M., Martin, A.P., 2015. Phytoplankton dynamics in contrasting early stage North Atlantic spring blooms: composition, succession, and potential drivers. Biogeosciences 12, 2395–2409.

Davis, C.E., Blackbird, S., Wolf, G., Sharples, J., Woodward, E. M. S., Mahaffey, C., this issue. Seasonal organic matter dynamics in a temperate shelf sea. Progr. Oceanogr.

Del Giorgio, P.A., Cole, J.J., 1998. Bacterial growth efficiency in natural aquatic systems. Annu. Rev. Ecol. Syst. 503–541.

Del Giorgio, P.A., Gasol, J.M., 2008. Physiological structure and single-cell activity in marine bacterioplankton. In: Kirchman, D.L. (Ed.), Microbial Ecology of the Oceans. John Wiley & Sons, Inc., pp. 243–298.

Ducklow, H., Kirchman, D., Quinby, H., Carlson, C., Dam, H., 1993. Stocks and dynamics of bacterioplankton carbon during the spring bloom in the eastern North Atlantic Ocean. Deep Sea Res. Part II 40, 245–263.

Falkowski, P.G., Owens, T.G., 1980. Light—shade adaptation two strategies in marine phytoplankton. Plant Physiol. 66, 592–595.

Falkowski, P.G., Raven, J.A., 2007. Aquatic Photosynthesis, second ed. Princeton University Press.

Fasham, M., Holligan, P., Pugh, P., 1983. The spatial and temporal development of the spring phytoplankton bloom in the Celtic Sea, April 1979. Prog. Oceanogr. 12, 87–145.

Fernández, E., Serret, P., De Madariaga, I., Harbour, D., Davies, A., 1992. Photosynthetic carbon metabolism and biochemical composition of spring phytoplankton assemblages enclosed in microcosms: the diatom-Phaeocystis sp. succession. Mar. Ecol. Prog. Ser. 90, 89–102.

Fileman, E.S., Fitzgeorge-Balfour, T., Tarran, G.A., Harris, R.P., 2011. Plankton community diversity from bacteria to copepods in bloom and non-bloom conditions in the Celtic Sea in spring. Estuar. Coast. Shelf Sci. 93, 403–414.

García-Martín, E.E., Aranguren-Gassis, M., Hartmann, M., Zubkov, M.V., Serret, P., 2016. Contribution of bacterial respiration to plankton respiration from 50 N to 44 S in the Atlantic Ocean. Prog. Oceanogr. http://dx.doi.org/10.1016/j.pocean.2016.11.006.

García-Martín, E.E., Daniels, C.J., Davidson, K., Davis, C.E., Mahaffey, C., Mayers, K.M.J., McNeill, S., Poulton, A.J., Purdie, D.A., Tarran, G., Robinson, C., this issue. Seasonal changes in microplankton respiration and bacterial metabolism in a temperate Shelf Sea. Prog Oceanogr (in rev).

Goldman, J.C., Caron, D.A., Dennett, M.R., 1987. Regulation of gross growth efficiency and ammonium regeneration in bacteria by substrate C:N ratio. Limnol. Oceanogr. 32, 1239–1252.

Grossart, H.-P., Czub, G., Simon, M., 2006. Algae–bacteria interactions and their effects on aggregation and organic matter flux in the sea. Environ. Microbiol. 8, 1074–1084.

Guillemette, F., Leigh McCallister, S., Del Giorgio, P.A., 2016. Selective consumption and metabolic allocation of terrestrial and algal carbon determine allochthony in lake bacteria. ISME J. 10, 1373–1382.

Henson, S.A., Robinson, I., Allen, J.T., Waniek, J.J., 2006. Effect of meteorological conditions on interannual variability in timing and magnitude of the spring bloom in the Irminger Basin, North Atlantic. Deep Sea Res. Part I 53, 1601–1615.

Hickman, A., Poulton, A.J., Mayers, K.M.J., Tarran, G.A., 2017;al., this issue. Seasonal variability in size-fractionated chlorophyll-a and primary production in the Celtic Sea. Prog. Oceanogr.

Humphreys, M.P., Moore, C.M., Achterberg, E.P., Hartman, S.E., Kivimäe, C., Griffiths, A.M., Smilenova, A., Chowdhury, M.Z.H., Hull, T., Woodward, E.M.S., Wihsgott, J., Hopkins, J.E., 2017;al., this issue. Mechanisms for a nutrient-conservative carbon pump in a seasonally stratified, temperate continental shelf sea. Prog. Oceanogr.

Hydes, D., Aoyama, M., Aminot, A., Bakker, K., Becker, S., Coverly, S., Daniel, A., Dickson, A., Grosso, O., Kerouel, R., 2010. Recommendations for the determination of nutrients in seawater to high levels of precision and inter-comparability using continuous flow analysers. GO-SHIP (Unesco/IOC).

Jiao, N., Robinson, C., Azam, F., Thomas, H., Baltar, F., Dang, H., Hardman-Mountford, N., Johnson, M., Kirchman, D., Koch, B., 2014. Mechanisms of microbial carbon sequestration in the ocean–future research directions. Biogeosciences 11, 5285–5306.

Joint, I., Owens, N., Pomroy, A., 1986. Seasonal production of photosynthetic picoplankton and nanoplankton in the Celtic Sea. Mar. Ecol. Prog. Ser. 28, 251–258.

Joint, I., Wollast, R., Chou, L., Batten, S., Elskens, M., Edwards, E., Hirst, A., Burkill, P., Groom, S., Gibb, S., 2001. Pelagic production at the Celtic Sea shelf break. Deep Sea Res. Part II 48, 3049–3081.

Kirchman, D., 2001. Measuring bacterial biomass production and growth rates from leucine incorporation in natural aquatic environments. In: Methods in Microbiology. Academic Press, pp. 227–237.

Lancelot, C., 1984. Extracellular release of small and large molecules by phytoplankton in the southern bight of the North Sea. Estuar. Coast. Shelf Sci. 18, 65–77.

Landa, M., Blain, S., Christaki, U., Monchy, S., Obernosterer, I., 2015. Shifts in bacterial community composition associated with increased carbon cycling in a mosaic of phytoplankton blooms. ISME J. 10, 39–50.

Legendre, L., Le Fèvre, J., 1995. Microbial food webs and the export of biogenic carbon in oceans. Aquat. Microb. Ecol. 9, 69–77.

Lemée, R., Rochelle-Newall, E., Van Wambeke, F., Pizay, M., Rinaldi, P., Gattuso, J., 2002. Seasonal variation of bacterial production, respiration and growth efficiency in the open NW Mediterranean Sea. Aquat. Microb. Ecol. 29, 227–237.

Li, W., Dickie, P., Harrison, W., Irwin, B., 1993. Biomass and production of bacteria and phytoplankton during the spring bloom in the western North Atlantic Ocean. Deep Sea Res. Part II 40, 307–327.

Lønborg, C., Martínez-García, S., Teira, E., Álvarez-Salgado, X.A., 2011. Bacterial carbon demand and growth efficiency in a coastal upwelling system. Aquat. Microb. Ecol. 63, 183–191.

Lønborg, C., Nieto-Cid, M., Hernando-Morales, V., Hernández-Ruiz, M., Teira, E., Álvarez-Salgado, X.A., 2016. Photochemical alteration of dissolved organic matter and the subsequent effects on bacterial carbon cycling and diversity. FEMS Microbiol. Ecol. 92, fiw048.

López-Sandoval, D., Fernández, A., Marañón, E., 2011. Dissolved and particulate primary production along a longitudinal gradient in the Mediterranean Sea. Biogeosciences 8, 815–825.

Maldonado, F., Packard, T., Gómez, M., 2012. Understanding tetrazolium reduction and the importance of substrates in measuring respiratory electron transport activity. J. Exp. Mar. Biol. Ecol. 434, 110–118.

Marra, J., 2002. Approaches to the measurement of plankton production. In: Williams, P.J. le B., Thomas, D.N., Reynolds, C.S. (Eds.), Phytoplankton Productivity - Carbon Assimilation in Marine and Freshwater Ecosystems. Blackwell Science, pp. 78–108.

Martínez-García, S., Fernández, E., Aranguren-Gassis, M., Teira, E., 2009. In vivo electron transport system activity: a method to estimate respiration in natural marine microbial planktonic communities. Limnol. Oceanogr.: Methods 7, 459–469.

Mayers, K.M.J., Poulton, A.J., Daniels, C.J., Wells, S.R., Woodward, E.M.S., Tyrrell, T., Giering, S.L.C., this issue. Top-down control of coccolithophore populations during spring in a temperate Shelf Sea (Celtic Sea, April 2015). Prog. Oceanogr.

Miller, J.C., Miller, J.N., 1988. Statistics for Analytical Chemistry, second ed. Ellis Horwood, Chichester.

Moore, C.M., Suggett, D.J., Hickman, A.E., Kim, Y.-N., Tweddle, J.F., Sharples, J., Geider, R.J., Holligan, P.M., 2006. Phytoplankton photoacclimation and photoadaptation in response to environmental gradients in a shelf sea. Limnol. Oceanogr. 51, 936–949.

Pedler, B.E., Aluwihare, L.I., Azam, F., 2014. Single bacterial strain capable of significant contribution to carbon cycling in the surface ocean. Proc. Natl. Acad. Sci. 111, 7202–7207.

Pingree, R., Holligan, P., Mardell, G., Head, R., 1976. The influence of physical stability on spring, summer and autumn phytoplankton blooms in the Celtic Sea. J. Mar. Biol. Assoc. UK 56, 845–873.

Poulton, A.J., Daniels, C.J., Esposito, M., Humphreys, M.P., Mitchell, E., Ribas-Ribas, M., Russell, B.C., Stinchcombe, M.C., Tynan, E., Richier, S., 2016. Production of dissolved organic carbon by Arctic plankton communities: responses to elevated carbon dioxide and the availability of light and nutrients. Deep Sea Res. Part II 127, 60–74.

Poulton, A.J., Davis, C.E., Daniels, C.J., Mayers, K.M.J., Harris, C., Tarran, G.A., Widdicombe, C.E., Woodward, E.M.S., 2017;al., this issue. Seasonal phosphorus dynamics in a temperate shelf sea (Celtic Sea): uptake, release, turnover and stoichiometry. Prog. Oceanogr.

Rees, A.P., Joint, I., Donald, K.M., 1999. Early spring bloom phytoplankton-nutrient dynamics at the Celtic Sea Shelf Edge. Deep Sea Res. Part I 46, 483–510.

Reinthaler, T., Herndl, G.J., 2005. Seasonal dynamics of bacterial growth efficiencies in relation to phytoplankton in the southern North Sea. Aquat. Microb. Ecol. 39, 7–16.

Rivkin, R.B., Anderson, M.R., 1997. Inorganic nutrient limitation of oceanic bacterioplankton. Limnol. Oceanogr. 42, 730–740.

Rivkin, R.B., Legendre, L., 2001. Biogenic carbon cycling in the upper ocean: effects of microbial respiration. Science 291, 2398–2400.

Robinson, C., 2008. Heterotrophic bacterial respiration. In: Kirchman, D.L. (Ed.), Microbial Ecology of the Oceans. John Wiley & Sons, Inc, pp. 299–334.

Robinson, C., Williams, P.J. le B., 1999. Plankton net community production and dark respiration in the Arabian Sea during September 1994. Deep Sea Res. Part II 46, 745–765.

Schlitzer, R., 2015. Ocean Data View. < http://odv.awi.de > .

Sherr, E., Sherr, B., 1994. Bacterivory and herbivory: key roles of phagotrophic protists in pelagic food webs. Microb. Ecol. 28, 223–235.

Sintes, E., Stoderegger, K., Parada, V., Herndl, G.J., 2010. Seasonal dynamics of dissolved organic matter and microbial activity in the coastal North Sea. Aquat. Microb. Ecol. 60, 85.

Smith, D.C., Steward, G.F., Long, R.A., Azam, F., 1995. Bacterial mediation of carbon fluxes during a diatom bloom in a mesocosm. Deep Sea Res. Part II 42, 75–97.

Smyth, T.J., Allen, I., Atkinson, A., Bruun, J.T., Harmer, R.A., Pingree, R.D., Widdicombe, C.E., Somerfield, P.J., 2014. Ocean net heat flux influences seasonal to interannual patterns of plankton abundance. PLoS ONE 9, e98709.

Stewart, J.C., Hawcroft, D.M., 1977. A Manual of Radiobiology. University of Washington Press, Seattle.

Tada, Y., Taniguchi, A., Nagao, I., Miki, T., Uematsu, M., Tsuda, A., Hamasaki, K., 2011. Differing growth responses of major phylogenetic groups of marine bacteria to natural phytoplankton blooms in the western North Pacific Ocean. Appl. Environ. Microbiol. 77, 4055–4065.

Tarran, G.A., Heywood, J.L., Zubkov, M.V., 2006. Latitudinal changes in the standing stocks of nano- and picoeukaryotic phytoplankton in the Atlantic Ocean. Deep Sea Res. Part II 53, 1516–1529.

Taylor, A.H., Geider, R.J., Gilbert, F.J., 1997. Seasonal and latitudinal dependencies of phytoplankton carbon-to-Chl a ratios: results of a modelling study. Mar. Ecol. Prog. Ser. 152, 51–66.

Teira, E., Hernando-Morales, V., Fernández, A., Martínez-García, S., Álvarez-Salgado, X., Bode, A., Varela, M., 2015. Local differences in phytoplankton–bacterioplankton coupling in the coastal upwelling off Galicia (NW Spain). Mar. Ecol. Prog. Ser. 528, 53–69.

Van Oostende, N., Harlay, J., Vanelslander, B., Chou, L., Vyverman, W., Sabbe, K., 2012. Phytoplankton community dynamics during late spring coccolithophore blooms at the continental margin of the Celtic Sea (North East Atlantic, 2006–2008). Prog. Oceanogr. 104, 1–16.

Wear, E.K., Carlson, C.A., James, A.K., Brzezinski, M.A., Windecker, L.A., Nelson, C.E., 2015. Synchronous shifts in dissolved organic carbon bioavailability and bacterial community responses over the course of an upwelling-driven phytoplankton bloom. Limnol. Oceanogr. 60, 657–677.

Widdicombe, C., Eloire, D., Harbour, D., Harris, R., Somerfield, P., 2010. Long-term phytoplankton community dynamics in the Western English Channel. J. Plankton Res. 32, 643–655.

Wihsgott, J.U., Sharples, J., Hopkins, J.E., Woodward, E.M.S., Greenwood, N., Hull, T., Sivyer, D.B., this issue. Investigating the autumn bloom's significance within the seasonal cycle of primary production in a temperate shelf sea. Prog Oceanogr. (in rev).

Williams, P.J. le B., del Giorgio, P.A., 2005. Respiration in aquatic ecosystems: history and background. In: del Giorgio, P.A., Williams, P.J. le B. (Eds.), Respiration in Aquatic Ecosystems. Oxford University Press, pp. 1–17.

Woodward, E.M.S., Rees, A., 2001. Nutrient distributions in an anticyclonic eddy in the northeast Atlantic Ocean, with reference to nanomolar ammonium concentrations. Deep Sea Res. Part II 48, 775–793.